ADVANCES IN ATMOSPHERIC SCIENCES, VOL. 31, MAY 2014, 637–646

The Relationship between the El Niño/La Niña Cycle and the Transition Chains of Four Atmospheric Oscillations. Part II: The Relationship and a New Approach to the Prediction of El Niño

PENG Jingbei*, CHEN Lieting, and ZHANG Qingyun

ICCES, Institute of Atmospheric Physics, Chinese Academy of Sciences, Beijing 100029

(Received 8 November 2012; revised 21 June 2013; accepted 11 July 2013)

ABSTRACT

The authors explored the connection and transition chains of the Northern Oscillation (NO) and the North Pacific Oscillation (NPO), the Southern Oscillation (SO), and the Antarctic Oscillation (AAO) on the interannual timescale in a companion paper. In this study, the connection between the transition chains of the four oscillations (the NO and NPO, the SO and AAO) and the El Niño/La Niña cycle were examined. It was found that during the transitions of the four oscillations, alternate anticyclonic/cyclonic correlation centers propagated from the Western Pacific to the Eastern Pacific along both sides of the equator. Between the anticyclonic/cyclonic correlation centers, the zonal wind anomalies also moved eastwardly, favoring the advection of sea surface temperature anomalies from the tropical Western Pacific to the Eastern Pacific. When the anticyclonic anomalies arrived in the Eastern Pacific, the positive phase of NO/SO and La Niña were established and vice versa. Thus, in 4-6 years, with an entire transition chain of the four oscillations, an El Niño/La Niña cycle completed. The eastward propagation of the covarying anomalies of the sea level pressure, zonal wind, and sea surface temperature was critical to the transition chains of the four oscillations and the cycle of El Niño/La Niña.

Based on their close link, a new empirical prediction method of the timing of El Niño by the transition chains of the four oscillations was proposed. The assessment provided confidence in the ability of the new method to supply information regarding the long-term variations of the ocean and atmosphere in the tropical Pacific.

Key words: the atmospheric oscillations, the oscillation transition, El Niño/La Niña cycle, El Niño prediction

Citation: Peng, J. B., L. T. Chen, and Q. Y. Zhang, 2014: The relationship between the El Niño/La Niña cycle and the transition chains of four atmospheric oscillations. Part II: The relationship and a new approach to the prediction of El Niño. *Adv. Atmos. Sci*., **31**(3), 637–646, doi: 10.1007/s00376-013-2279-9.

1. Introduction

The Northern Oscillation (NO) and the Southern Oscillation (SO) reflected the out-of-phase variations of Sea Level Pressure Anomalies (SLPAs) between the Eastern and Western Pacific. The North Pacific Oscillation (NPO) and the Antarctic Oscillation (AAO) were the oscillations between the subtropics and the high and mid-latitudes in the North and South Pacific, respectively. The NO, NPO, SO, and AAO (hereafter referred as the four oscillations) were the leading modes of the interannual variations of the low-level circulation over the North and South Pacific. In the companion paper, Peng et al. (2014, hereafter referred to as Part I) documented the connections and transition chains of the four oscillations on an interannual timescale.

(1) In 4–6 years, one oscillation transitioned to another following the general pattern of the transition chain of NO and NPO from the negative phase of the NO (NO^-) to the positive phase of the NPO (NPO^+), then the NO^+, the NPO^-, and the NO^- ($NO^- \rightarrow NPO^+ \rightarrow NO^+ \rightarrow NPO^- \rightarrow NO^-$). The general pattern of the transition chain of the SO and AAO was similar to that for the NO and NPO, namely, $SO^- \rightarrow AAO^+ \rightarrow SO^+ \rightarrow AAO^- \rightarrow SO^-$. The beginning and the end of the transition chains of oscillations in the North and South Pacific was roughly simultaneous.

(2) The major feature of the low-level circulation evolution during the transition chains of the four oscillations was the eastward propagation of alternate positive/negative SLPAs along both sides of the equator. During the transition between the NO and the NPO, the SLPAs propagated eastwardly along the tropic Pacific, and out-of-phase SLPAs propagated northwestwardly from the Eastern Pacific toward the Aleutian region. In the South Pacific, the SLPAs in the mid- and high-latitudes were out of phase with those in the tropical Pacific Ocean, causing the transition between the SO and the AAO.

Each member of the four oscillations connected with El

* Corresponding author: PENG Jingbei
Email: pengjingbei@mail.iap.ac.cn

Niño/La Niña (EN/LN) closely (Bjerknes, 1969; Chen, 1982; Vimont et al., 2003; Carvalho et al., 2005). Case studies indicated that the transition chains of the four oscillations connected to the EN/LN cycle (Wu and Chen, 1995). The general connection between the transition chains and the EN/LN cycle is unclear.

There are many dynamic and statistical models available to predict EN/LN because of its importance to the seasonal forecast. It is still difficult to predict the occurrence of EN by several months due to the complexity of EN (Landsea and Knaff, 2000; Clarke and van Gorder, 2003; Dominiak and Terray, 2005). For example, in the spring 2011, the LN condition had finished. Many models predicted there would be a warm phase in the summer or fall of 2011[a]. Some models showed different results: that the LN condition would return in fall 2011 and persist into 2012. It is therefore necessary to develop new approaches to predict EN. Using the transition chains of the four oscillations may be a reasonable way to predict EN.

In this study, we discuss the general connection between the EN/LN cycle and the transition chains of the four oscillations. We also demonstrate a new empirical method to forecast the timing of the EN event by the phase spaces that describe the transitions of the four oscillations. Section 2 describes the data and the methods of analysis. Section 3 presents the linkage between the transition chains of the four oscillations and the EN/LN cycle. Section 4 discusses a new approach to long-term prediction of the onset of EN. The final section contains the discussion and conclusions.

2. Data and methods

2.1. *Data and the indices of the four oscillations*

To study the connections between the EN/LN cycle and the transition chains of the four oscillations, we used the following data: (1) the monthly SSTA from the Kaplan Extended SSTA data set version 2.0 on a $5^\circ \times 5^\circ$ grid (Kaplan et al., 1998); (2) the anomalies of wind over 1000 hPa ($\boldsymbol{V}'_{1000}$) and SLP data from the National Centers for Environmental Prediction-National Center for Atmospheric Research (NCEP-NCAR) reanalysis that were available on a $2.5^\circ \times 2.5^\circ$ grid (Kalnay et al., 1996). We also used monthly SSTA data from the Niño3 region (5°S–5°N and 90°W–150°W, hereafter, denoted as Niño-3) to identify the EN/LN events. All of the data were from 1951 to 2011. Monthly anomalies were computed for long-term monthly means defined over the 61-year record.

The four oscillations were the leading modes of the low-level circulation over the Pacific Basin (Peng et al., 2014, Part I). Thus, we applied empirical orthogonal functions (EOFs) to the interannual variation of the SLPAs in the North (0°–60°N, 100°E–80°W) and South Pacific region (80°S–0°, 50°E–80°W). The first two modes of the North (South) Pacific were similar to NO and NPO (SO and AAO), respectively (Peng et al., 2014, Fig. 3), and the time series were statistically significantly related to the corresponding oscillation index (Peng et al., 2014, Table 1). The EOF modes were related to the physical modes through the correlation of the time series and spatial patterns. Thus, we used the first two principal components of the SLPAs in the North Pacific region (hereafter referred to as the NPC1 and the NPC2) to represent the NOI and the NPOI and the first two principal components in the South Pacific region (the SPC1 and the SPC2) to represent the SOI and the AAOI, respectively.

2.2. *The identification of the EN and LN events*

EN and LN were identified by the definition of the State Oceanic Administration of the People's Republic of China. The onset of an EN (LN) episode such as Niño-3 exceeds + (−) 0.5°C and lasts for at least 6 months, allowing a 3 month break. A total of 13 EN and 12 LN events (Table 1) were identified in the period of 1951–2011. The month of the maximum (minimum) of Niño-3 was denoted as the peak time of the EN (LN) event.

2.3. *Methods*

The significant interannual periods of the four oscillations and the EN/LN cycle were 3–7 years (Rasmusson and Carpenter, 1982; Part I). A second-order Butterworth bandpass filter was used to remove the short-term and interdecadal variations (Li, 1991). The data were normalized before applying the bandpass filter to highlight the variability in the tropics.

A cross-time-lagged correlation analysis was used to discuss the atmospheric and oceanic evolutions. The level of significance of the time-lag correlation is estimated by the Monte Carlo approach (Livezey and Chen, 1983; Shi et al., 1997).

Phase space is an M-dimensional Euclidean space whose coordinates describe the state of a system (Lorenz, 1963). The orbit of the trajectory in the phase spaces spanned by NPC1-NPC2 and SPC1-SPC2 represents the transition chains among the four oscillations (Peng et al., 2014, Part I). It is convenient to use phase space to discuss the relationship between the EN/LN cycle and the transition chains of the four oscillations and to establish the prediction model of the onset of EN events. The brief introduction and reconstruction of phase space was detailed in section 2.2 of Part I.

3. The linkage between the transition chains of the four oscillations and the EN/LN cycle

We correlated the interannual variation of NOI (NPC1) against $\boldsymbol{V}'_{1000}$ and SSTA (Fig. 1). This allowed for us to visualize the slow eastward propagation of cyclonic/anticyclonic anomalies, zonal wind anomalies, and SSTAs in the tropical Pacific associated with the transition chains of the four oscillations. The maximum time lag was 30 months to cover the period of the transition chains of the four oscillations (4–6 years). We defined the NO leading $\boldsymbol{V}'_{1000}$ and SSTAs at 30 months as month −30 and the zero-lag as month 0. The

[a]http://www.cpc.ncep.noaa.gov/products/analysis_monitoring/lanina/enso_evolution-status-fcsts-web.pdf

Table 1. The EN and LN episodes and peak time based on Niño-3 during 1951–2011.

EN	Peak time	LN	Peak time
Jul 1951–Dec 1951	Nov 1951	Apr 1954–Jan 1956	Nov 1955
Jun 1957–Mar 1958	Dec 1957	Sep 1962–Feb 1963	Dec 1962
Jul 1963–Dec 1963	Dec 1963	Apr 1964–Jan 1965	May 1964
May 1965–Feb 1966	Dec 1965	Aug 1967–May 1968	Feb 1968
Dec 1968–Jan 1970	Dec 1969	May 1970–Jan 1972	Jul 1970
May 1972–Feb 1973	Dec 1972	Apr 1973–Apr 1976	Jan 1976
Jul 1976–Jan 1977	Oct 1976	May 1984–Feb 1986	Dec 1984
May 1982–Aug 1983	Dec 1982	Apr 1988–May 1989	Dec 1988
Oct 1986–Dec 1987	Sep 1987	May 1995–Jun 1996	Nov 1995
Oct 1991–May 1992	Dec 1991	Sep 1998–Jan 2001	Jan 2000
May 1997–May 1998	Dec 1997	May 2007–Mar 2008	Nov 2007
Jun 2002–Jan 2003	Nov 2002	Jun 2010–Mar 2011	Oct 2010
Jun 2009–Apr 2010	Dec 2009		

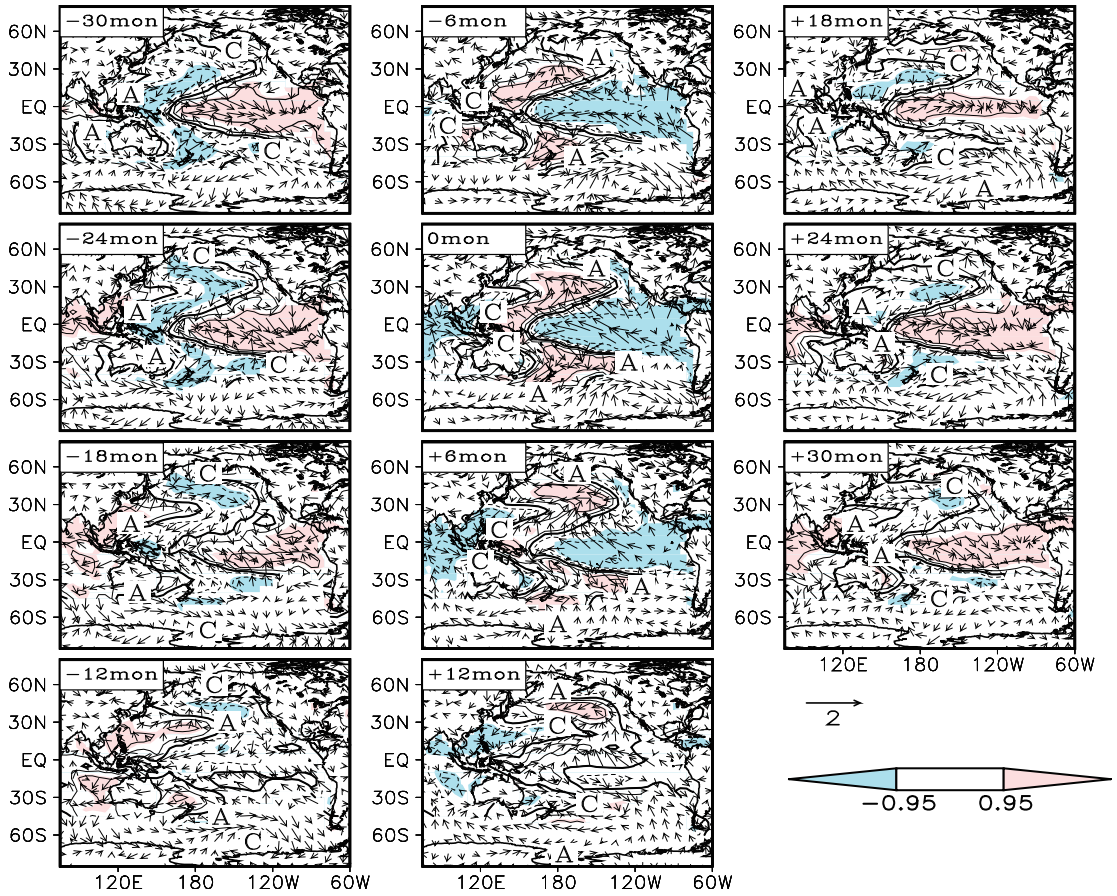

Fig. 1. The cross correlation between the interannual NOI (NPC1) and interannual SSTAs (contour) and $\boldsymbol{V}'_{1000}$ (vector) over the Pacific domain from 1951 to 2006 with a maximum lag of 30 months. The red (blue) shaded area indicates that the positive (negative) correlations were significant at the 95% confidence level. A represents an anticyclonic anomaly, and C represents a cyclonic anomaly. The thick solid line is the zero line.

characteristics of circulation and SSTA evolutions revealed by different oscillation indices were similar to each other, only differing by a time delay.

At month −30, there were two pairs of cyclonic and anticyclonic correlation centers located at each side of the equator over the tropical Pacific. The anticyclonic correlation centers were around the Philippines and west to Australia, which were identified by the letter "A". The cyclonic correlation centers over the Northeast and Southeast Pacific were identified by the letter "C". This correlation pattern corresponded to one for an extreme NOI and SOI period, namely, NO^-/SO^- (NO^+/SO^+). In contrast, the positive SST correlations occupied the tropical Eastern Pacific, and the negative SST correlations of a horseshoe shape emanated from the

equator near the date line to the North and South American coasts. This pattern was nearly symmetric about the equator. It reflected the mature phase of EN (LN).

From month −24 to −12, the anticyclonic correlation pair moved eastward. Between the anticyclonic correlation pair, there were negative zonal wind correlations in the tropical Pacific. The tropical zonal wind anomalies favored cold (warm) advection from the Western to the Central Pacific (Gill, 1983; Schiller et al., 2000; Vialard et al., 2001). At month −12, the anticyclonic correlation pair, the negative zonal wind correlations, and the negative SST correlations arrived at the Central Pacific. Furthermore, the cyclonic correlation centers were from the tropical Eastern Pacific and propagated along the western shore of North America over the Aleutian area, and those from the Southern Indian Ocean arrived at the Southeastern Pacific at approximately 65°S. The NO^-/SO^- (NO^+/SO^+) transitioned to the NPO^+/AAO^+(NPO^-/AAO^-). EN (LN) decayed.

At month 0, the two moving anticyclonic correlation centers arrived at the Eastern Pacific, and the Western Pacific where the originally anticyclonic correlation centers were located was occupied by two new cyclonic correlation centers. The negative SST correlations were large and widely spread in the tropical Eastern Pacific. At this time, the correlation patterns of the wind field and SST became nearly identical to those from approximately 24 months ago, but reversed in sign. This means that the NO^+/SO^+ (NO^-/SO^-) and LN (EN) were established.

In the next 2 to 3 years, the cyclonic correlation centers over the Western Pacific also moved eastward, along with the positive zonal wind and SST correlation in the tropical Pacific. At approximately month +24, the cyclonic correlation centers arrived in the Eastern Pacific. The NO^-/SO^- (NO^+/SO^+) and EN (LN) were restored.

From the above analyses, it can be concluded that the transition chains of the four oscillations connected closely with the EN/LN cycle. The eastward propagation of cyclonic/anticyclonic pairs across the equator which was critical to the transition chains of the four oscillations led to the eastward propagation of the tropical zonal wind anomaly and the SSTA signals. As alternate anticyclonic/cyclonic correlation centers propagated from the Western Pacific to the Eastern Pacific along both sides of the equator during the transition chains of the four oscillations, the zonal wind anomalies between the anticyclonic/cyclonic correlation centers also moved eastwardly, favoring the advection of SSTA from the tropical Western Pacific to the Eastern Pacific. When the anticyclonic anomalies moved into the Eastern Pacific, the NO^+/SO^+ (NO^-/SO^-) and LN (EN) were established; conversely, the NO^-/SO^- (NO^+/SO^+) and EN (LN) occurred when the cyclonic anomalies located over the Western Pacific arrive in the Eastern Pacific. To assess the connection between the EN/LN cycle and the transition chains of the four oscillations, the time-longitude diagrams of SLPAs, SSTAs, and tropical zonal wind anomalies from May 1995 to April 2000 were shown in Fig. 2. The eastward propagation of

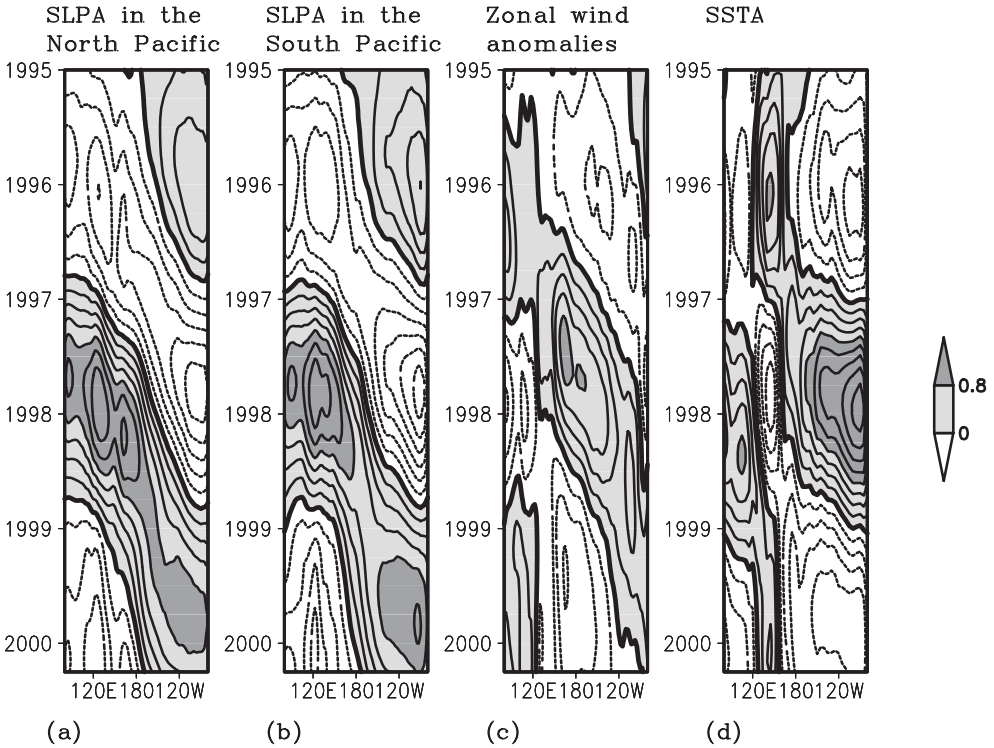

Fig. 2. Averaged time–longitude diagram in the tropical Pacific (10°N–10°S) for the normalized interannual SLPAs in the (a) tropical North (10°N–0°) and (b) South (0°–10°S) Pacific, (c) Zonal wind anomalies over 1000 hPa and (d) SSTAs from January 1995 to April 2000. The thick line is the zero line. The contour interval is 0.2. Positive anomalies are shaded.

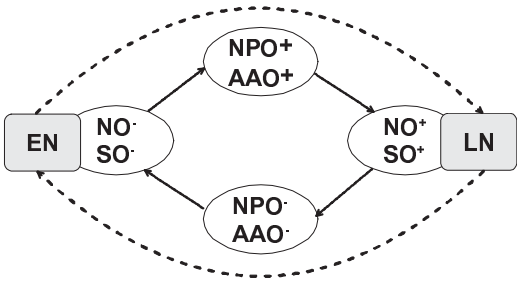

Fig. 3. Schematic diagram of the connections between the EN/LN cycle and the transitions of the four oscillations.

the SLPAs, tropical zonal wind anomalies, and SSTAs was evident. In addition, our results resembled the lag correlations between SSTAs in the eastern equatorial Pacific and global 1000 hPa geopotential height anomalies (Chen and Fan, 1993, Fig. 4). In the transition chains of the four oscillations ($NO^- \rightarrow NPO^+ \rightarrow NO^+ \rightarrow NPO^- \rightarrow NO^-$ and $SO^- \rightarrow AAO^+ \rightarrow SO^+ \rightarrow AAO^- \rightarrow SO^-$), an EN/LN cycle (EN → LN → EN) completed, as diagrammed schematically in Fig. 3.

4. A statistical prediction method of EN events using the transition chains of the four oscillations

The close connection between the EN/LN cycle and the transition chains of the four oscillations implied that it may be used in the EN prediction exercises. We plotted the peak time of all of the EN and LN events in the phase space spanned by NOI-NPOI and SOI-AAOI. The peak of each EN event was in the second or the third quadrant of the phase spaces, and LN was in the first or the fourth quadrant (figures not shown). This is consistent with the correspondence of EN (LN) to the NO^-/SO^- (NO^+/SO^+). Furthermore, from 1951 to 2006, there were 11 complete transition chains of NO and NPO (SO and AAO, Part I, Table 2) and 11 EN and 10 LN events. Each transition chain contains one EN event. Most transition chains and LN events were one-to-one, except the one from the spring of 1959 to the summer of 1965, with two LN events of 1962–63 and 1964–65, and the one from the winter of 1988/89 to the spring of 1995 with no LN. The difference between EN and LN events may be due to their asymmetry (An and Jin, 2004). Because of the complexity of the LN events, we focused on the possibility of predicting the timing of the EN events by the phase space. In this section, the prediction model was constructed using the data from 1951 to 1990.An assessment of the prediction ability was then conducted by forecasting four EN events after 1990.

Table 2. The time intervals between the onset of EN and Point A2 or Point B (T_{1N} and T_{1S}) and Point C (T_{2N} and T_{2S}) in the phase spaces of the North and South Pacific from 1952–90. Numbers in bold indicate the final predictors. * and ** mark the maxima and minima of T_{1S} and T_{2N}, respectively. Unit: month.

The beginning of EN	T_{1N}	T_{2N}	T_{1S}	T_{2S}
April 1957	8	**2**	**19**	4
July 1963	15	**4**	**14**	0
May 1965	10	**4**	**12****	8
December 1968	17	**4**	**14**	6
April 1972	10	**2**	**16**	5
June 1976	15	**1****	**16**	2
May 1982	13	**2**	**12****	3
October 1986	20	**5***	**21***	7
Average	13.50	**3.00**	**15.80**	4.38
Variance	4.04	**1.10**	**2.05**	2.67

4.1. *The prediction model construction*

Three critical points in the phase spaces were focused on construct the prediction model:

Point A: the flex point in the first (Point A1) or the fourth quadrants (Point A2) of the phase space.

Point B: the point when the orbit entered the fourth quadrant of the phase space.

Point C: the point when the orbit entered the third quadrant of the phase space.

The positions of the four time points in the phase space from August 1964 to May 1968 and December 1994 to January 1999 were marked in Fig. 4. Different points represented different patterns of SLPAs and zonal wind anomalies (Fig. 5). Point A represented the peak of the NO^+ (SO^+), namely, the beginning of the transition to NO^- (SO^-). The cross-equatorial tropical cyclone pairs and westerly anomalies prevailed over the Western Pacific (Figs. 5a and b). Point B was the point when the NPO^+ (AAO^+) transitioned to the NPO^- (AAO^-), and the negative SLPAs and westerly anomalies reached the Western and Central Pacific at Point B (Fig. 5c). Point C represented the time when the NO^+ (SO^+) transitioned to the NO^- (SO^-). The maxima of negative SLPAs and westerly anomalies were found in the vicinity of the date line (Fig. 5d). This was similar to the patterns in the development phase of EN (Wang, 1995). It is noted that Point A1 and A2 corresponded to different phases of NPO (AAO). Point A1 corresponded to NPO^+ (AAO^+), whereas Point A2 corresponded to NPO^- (AAO^-). This implied that the negative SLPAs and westerly anomalies at Point A2 (Fig. 5b) had reached a position east of those at Point A1 (Fig. 5a). It would take less time for the negative SLPAs and westerly anomalies at Point A2 to cross the Pacific Ocean than those in the case of Point A1. Thus, because Point A was in the first quadrant, namely, Point A1, we would take Point B into account rather than Point A.

We defined the time intervals between the onset of EN and Point A2 or Point B as T_{1N} (T_{1S}) and of Point C as T_{2N} (T_{2S}) in the phase space spanned by NOI-NPOI (SOI-AAOI). The results are shown in Table 2. Because the indices of the four oscillation began in 1951, the EN in 1951 was excluded. The variance of T_{1S} was 2.05 months, smaller than the one of T_{1N} for the North Pacific. In contrast, the variance of T_{2N} was smaller. It was 1.01 months. Thus, T_{1S} and T_{2N} were used to

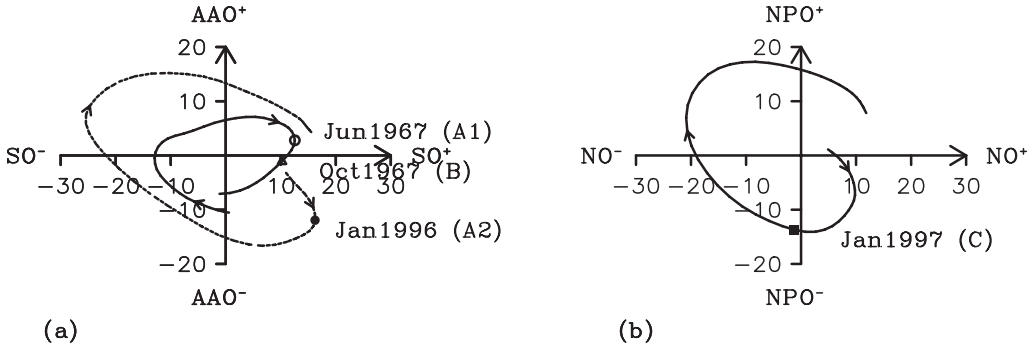

Fig. 4. (a) Two-dimensional phase portrait on the (SPC1, SPC2) plane, from August 1964 to May 1968 (solid line) and from December 1994 to January 1999 (dashed line) with the position of Point A1 (circle), Point A2 (dot), and Point B (triangle). (b) Two-dimensional phase portrait on the (NPC1, NPC2) plane from December 1994 to January 1999 with the position of Point C (closed square).

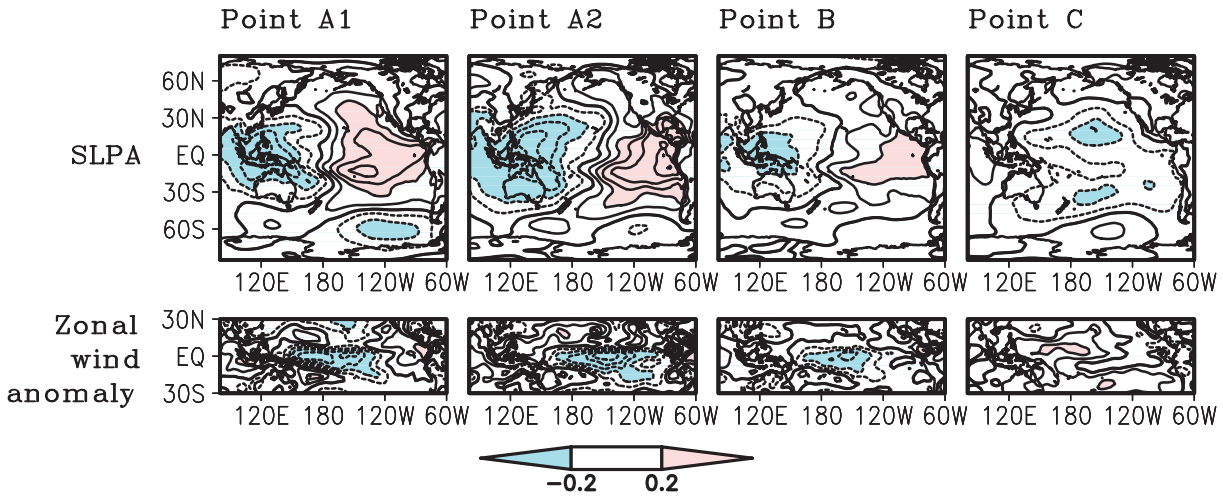

Fig. 5. The composite of the normalized interannual variations of SLPAs (top) and Zonal wind anomalies (bottom) associated with Point A1 (the first column), Point A2 (the second column), Point B (the third column), and Point C (the right column). The shading is explained in the legend. The thick solid line is zero line.

predict the timing of EN, shown in the bold letter columns in Table 2. Based on the above discussion, two time predictors were ultimately defined in the following way:

$$\begin{cases} T_{1S} = \begin{cases} \Delta t_{\text{from Point A in the phase space of SOI}-\text{AAOI to the onset of EN}}, & \text{in the case of Point A2} \\ \Delta t_{\text{from Point B in the phase space of SOI}-\text{AAOI to the onset of EN}}, & \text{in the case of Point A1} \end{cases} \\ T_{2N} = \Delta t_{\text{from Point C to the onset of EN, in the phase space of NOI}-\text{NPOI}} \end{cases}.$$

The maxima of T_{1S} was 21 months (in the forth column of Table 2, marked by *). The minima of T_{1S} was 12 months (marked by **). The average of T_{1S} was 13.50 months. Most of T_{1S} (6/8) was concentrated in 12–18 months. The maxima of T_{2N} was 5 months (in the third column of Table 2, also marked by *). The minima of T_{2N} was 1 month (marked by **). The average of T_{2N} was 3.6 months. Most of T_{2N} (7/8) was concentrated in 2–6 months. Thus, the timing of the onset of EN could be predicted by the following:

(1) when the orbit of trajectory in the South Pacific reached its flex point in the fourth quadrant or the orbit entered the fourth quadrant (Point A2 or Point B), the onset of an EN event would occur in 1–1.5 years;

(2) when the orbit of the trajectory in the North Pacific entered the third quadrant (Point C), an EN event would begin in 2-6 months.

4.2. *The assessment*

The performance of this method was evaluated by predicting four EN events after 1990. For the EN of 1991/1992, Point A appeared in the first quadrant. Thus, Point B (marked by a red triangle in Fig. 6a) was taken into account. Point B appeared in May 1990. This implied the onset of EN would be in the period from May–November 1991 (Table 3). The orbit reached Point C (marked by a red square in Fig. 6b) in February 1991. This predicted that the EN would begin in the

Table 3. The prediction of the onset time of two ENs after 1990 by the transition chains of the four oscillations.

Point A2 or B in the South Pacific		Point C in the North Pacific		Final Prediction of the timing of the onset of EN	The observational timing of the EN onset	Error (Units: month)
Date	prediction by T_{1S}	Date	prediction by T_{2N}			
May 1990	May–November 1991	February 1991	April–August 1991	Late summer–Autumn 1991	Oct 1991	1–2
January 1996	January–June 1997	January 1997	March–June 1997	Late Spring–Summer 1997	May 1997	1–2
March 2000	March–September of 2001	September 2001	November 2001–March 2002	Autumn 2001–Winter 2001/02	June 2002	5–6
December 2007	January–July 2009	October 2008	January–March 2009	Winter 2008/09–Early Spring 2009	June 2009	1–3

period from April to August 1991. Thus, the final prediction was that the beginning of the EN would be later summer to autumn of 1991. The observational EN beginning was October 1991. The difference between observation and prediction was approximately 1–2 months.

For the EN in 1997/98, Point A2 (marked by a red dot in Fig. 6a) appeared in January 1996, and the predicted EN onset time was from January to June 1997. Point C (marked by a red square in Fig. 6b) appeared in January 1997, and the predicted EN onset was from March to June 1997. Thus, the final prediction was that the EN episode would begin at the later spring of 1997. Observationally, the EN episode began in May 1997. The difference between the observation and prediction was approximately 1–2 months.

For the EN in 2002–03, Point B (a red triangle in Fig. 6c) appeared in March 2000, and Point C (a red square in Fig. 6d) appeared in September 2001. This implied that the onset of EN would be in the period from late spring to early autumn 2001 (Table 3). In fact, EN began in June 2002. The difference between observation and prediction was approximately 5–6 months. The large difference may be because the observational T_{1S} and T_{2N} were 27 and 10 months in this EN, which were the longest ones in the period of 1951–2011.

For the EN in 2009–10, Point A2 (marked by a red dot in Fig. 6c) appeared in December 2007, and Point C (marked by a red square in Fig. 6d) appeared in October 2008. The final prediction was that the EN episode would begin in winter 2008/09 or the early spring of 2009. Observationally, the EN episode began in June 2009. The difference between the observation and prediction was approximately 1–3 months. It was noticeable that the predicted onsets of the two ENs after 2000 were ahead of the actual onsets. This may be due to the interdecadal variation of the trade wind and thermocline depth in the Pacific Basin (Hu et al., 2012). After 2000, the trade wind was enhanced and the thermocline slope became steeper. This may weaken the eastward extension of the warm pool of the Western Pacific. In addition, the decrease in the variation of the warm water in the tropical Pacific may lead to La Niña-like background and weaker EN after 2000 (McPhaden, 2012).

In this section, we established a long-term empirical model to predict the onset of EN 1 to 1.5 years in advance using the phase orbit in the (SOI, AAOI) and (NOI, NPOI) plane. The assessment showed that it was confident for the new method to supply the information of long-term prediction of the onset of EN.

5. Discussions and Conclusion

We discussed the relationship between the EN/LN cycle and the transition chains of the four oscillations. As an EN/LN cycle completed, the four oscillations transitioned as follows: $SO^- \rightarrow AAO^+ \rightarrow SO^+ \rightarrow AAO^- \rightarrow SO^-$ and $NO^- \rightarrow NPO^+ \rightarrow NO^+ \rightarrow NPO^- \rightarrow NO^-$. We attempted to use these observational facts to monitor and predict the onset of EN.

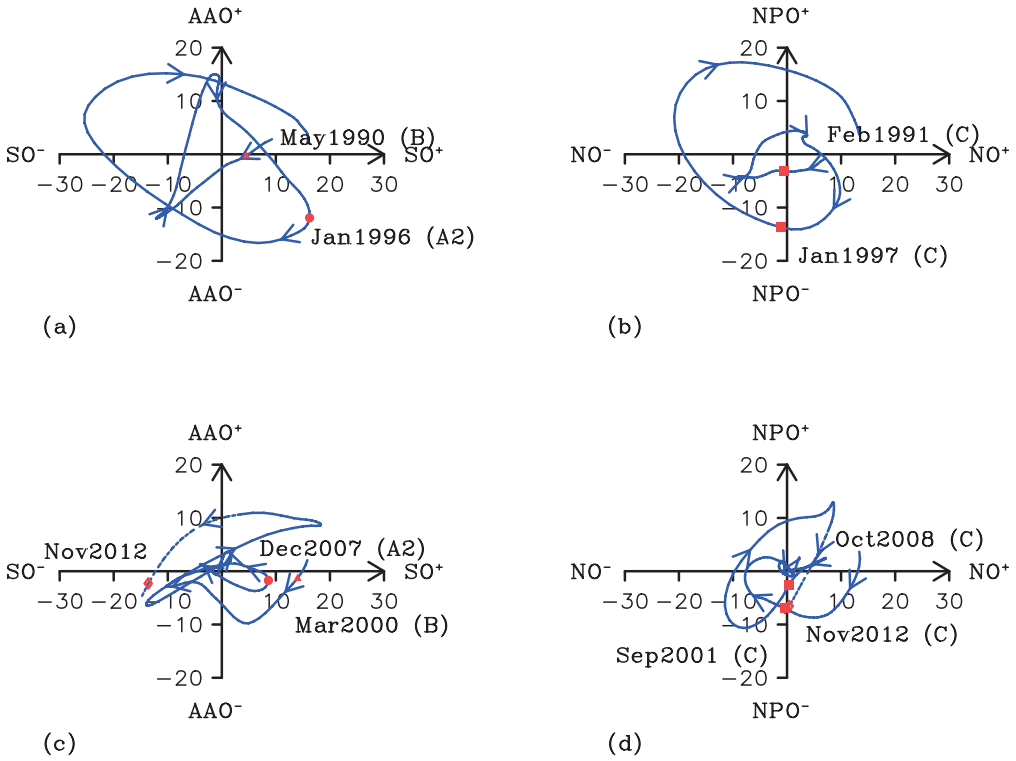

Fig. 6. Two-dimensional phase portraits on the (SPC1, SPC2) plane (a) and on the (NPC1, NPC2) plane (b) from January 1990 to November 1999. (c) and (d) are the same as (a) and (b) but from December 1999 to December 2012. The dashed lines denoted the phase portraits from January to December 2012. In (a) and (c), the red dots represented Point A2 in January 1996 and December 2007, and the red triangles represented Point B in May 1990 and March 2000. The red squares in (b) and (d) were for Point C. The red diamonds in (c) and (d) denote the positions of November 2012 and Point C in December 2012.

The connection between the EN/LN cycle and the transition chains of the four oscillations was the result of air-sea interaction (Peng et al., 2014, Part I). Previous studies showed that during the EN event, the zonal circulation in the mid-and high-latitude area developed. The anomalous easterlies and the so-called "cross-equatorial tropical anticyclone pairs" prevailed over the tropical western Pacific. NO and SO were in their negative phase. As EN transitioned to LN, the zonal circulation in the mid- and high latitudes weakened and the meridional circulation strengthened. The Aleutian Low deepened and the highs in the vicinity of the dateline enhanced (Zong, 2007). Moreover, the easterly anomalies in the tropical Pacific favored the eastern advection of cold sea surface temperature anomalies from the tropical Western Pacific. Due to the ocean-atmosphere coupling progress, the cold SSTAs and the anticyclone pairs propagated eastwardly (Tourre and White, 1997; Weisberg and Wang, 1997). As the anticyclone pairs arrived at the middle tropical Pacific, NO^- transitioned to NPO^+. Over the southern oceans, due to the feedback between the Antarctic Circumpolar Wave and the EN (White et al., 2002), the eastward propagation of cyclone anomalies may lead to the transition between SO and AAO. As the anticyclone pairs and negative SSTAs arrived at the eastern Pacific, EN transitioned into LN, and the negative phase of NO and SO transitioned into their positive phase. The sequent evolution of the atmosphere and ocean were similar, but reversed in sign. Thus, in 4–6 years, with an entire transition chain of the four oscillations, an El Niño/La Niña cycle completes.

Because of their close connection, the transition chains of the four oscillations could be used to construct a new empirical model to predict the timing of EN events. The statistical results showed that an EN episode was likely to begin in 1) 1 to 1.5 years after the AAO^+ transitioned to the AAO^- or the SO^+ reached its peak, 2) two to six months after the NO^+ transitioned to the NO^-. The assessment provided confidence in the ability of the new method to supply information regarding the long-term variations of the ocean and atmosphere in the tropical Pacific.

In fact, this empirical model can supply not only quantitate information on the onset of EN but also qualitative information on LN. For example, in the spring of 2010, the phase point on the (SOI, AAOI) plane was in the first quadrant. It was unlikely that the NO^+ and SO^+ would transition to the NO^- and SO^- very soon. The cold phase could last for another year. This prediction was identical to the observation.

However, the results were preliminary. The theoretical basis and prediction skill need to be improved. Figure 6

showed that the speed with which the orbit of the trajectory rotated around the origin of the phase space (equivalent to SLPA propagation speed) were different from one to another. As we mentioned before, the oceanic and atmospheric background state may influence the evolution of EN/LN. This empirical model only took interannual variations into account. The lack of interdecadal variation may affect the prediction skill. Furthermore, the key factors of each transition chain may not the same, leading to the uncertainty of the prediction. For example, if we extended the data to the end of 2012, Point C appeared at the end of 2012 (marked by a red diamond in Fig. 6d), implying that there will be an EN event in the summer of 2013. We also observed that the phase point had travelled from the first to the third quadrant through the second quadrant of the SOI-AAOI plane since the summer of 2010. This was not the classical Point B or Point A2 (Fig. 6c). That increased the uncertainty of the prediction. However, the interannual variation of SO and NO were both in their negative phase. It is unlikely that there will be an LN event in 2013. The Climate Prediction Center of the National Oceanic and Atmospheric Administration and the Japan Agency for Marine-Earth Science and Technology both predicted that the negative SSTAs in the eastern Pacific would start decaying in the coming spring and that EN-neutral conditions would last through the fall of 2013. The inclusion of interdecadal variations and the identification of key processes may improve the understanding of the mechanism of EN/LN and the atmospheric oscillations and the accuracy of this new prediction method.

In addition, filtering often results in lost points near the series endpoints. A new filtering method (Arguez et al., 2008) that retains the endpoint intervals needs to be used to improve the prediction skill of our method.

Acknowledgements. The authors are grateful to Professor JI Liren, Professor SUN Shuqing, and two anonymous reviewers' constructive suggestions, which improved the manuscript substantially. This work was supported by the National Key Technologies R&D Program of China (Grant No. 2009BAC51B02) and the National Basic Research Program of China (Grant NO. 2012CB957803).

REFERENCES

An, S.-I., and F.-F. Jin, 2004: Nonlinearity and asymmetry of ENSO. *J. Climate*, **17**, 2399–2412.

Arguez, A., P. Yu, and J. J. O'Brien, 2008: A new method for time series filtering near endpoints. *J. Atmos. Oceanic Technol.*, **25**(4), 534–546, doi: 10.1175/2007JTECHA924.1.

Bjerknes, J., 1969: Atmospheric teleconnections from the equatorial Pacific. *Mon. Wea. Rev.*, **97**, 163–172.

Carvalho, L. M. V., C. Jones, and A. Tercio, 2005: Opposite phases of the antarctic oscillation and relationships with intraseasonal to interannual activity in the tropics during the Austral Summer. *J. Climate*, **18**, 702–718.

Chen, L. T., 1982: Interaction between the subtropical High over the North Pacific and the sea surface temperature of the eastern equatorial Pacific. *Scientia Atmospherica Sinica*, **6**, 148–156. (in Chinese)

Chen, L. T., and Z. Fan, 1993: The Southern Oscillation/Northern Oscillation cycle associated with sea surface temperature in the equatorial Pacific. *Adv. Atmos. Sci.*, **10**, 353–364.

Clarke, A. J., and S. van Gorder, 2003: Improving El Niño prediction using a space-time integration of Indo-Pacific winds and equatorial Pacific upper ocean heat content. *Geophys. Res. Lett.*, **30**, doi: 10.1029/2002GL016673.

Dominiak, S., and P. Terray, 2005: Improvement of ENSO prediction using a linear regression model with a southern Indian Ocean sea surface temperature predictor. *Geophys. Res. Lett.*, **32**, doi: 10.1029/2005GL023153.

Gill, A. E., 1983: An estimation of sea-level and surface-current anomalies during the 1972 El Niño and consequent thermal effects. *J. Phys. Oceanogr.*, **13**, 586–606.

Hu, Z.-Z., A. Kumar, H.-L. Ren, H. Wang, M. L'Heureux, and F.-F. Jin, 2012: Weakened interannual variability in the tropical Pacific Ocean since 2000. *J. Climate*, **26**, 2601–2613, doi: 10.1175/JCLI-D-12-00265.1.

Kalnay, E., and Coauthors, 1996: The NCEP/NCAR 40-year reanalysis project. *Bull. Amer. Meteor. Soc.*, **77**, 437–471.

Kaplan, A., M. A. Cane, Y. Kushnir, A. C. Clement, M. B. Blumenthal, and B. Rajagopalan, 1998: Analyses of global sea surface temperature 1856–1991. *J. Geophys. Res.*, **103**, 18 567–18 589.

Landsea, C. W., and J. A. Knaff, 2000: How much skill was there in forecasting the very strong 1997–98 El Nino? *Bull. Amer. Meteor. Soc.*, **81**, 2107–2119.

Li, C. Y., 1991: *Low-frequency Oscillation in the Atmosphere*. China Meteorological Press, 12–18. (in Chinese)

Livezey, R. E., and W. Y. Chen, 1983. Statistical field significance and its determination by Monte Carlo techniques. *Mon. Wea. Rev.*, **111**, 46–59.

Lorenz, E. N., 1963: Deterministic nonperiodic flow. *J. Atmos. Sci.*, **20**, 130–141.

McPhaden, M. J., 2012: A 21st century shift in the relationship between ENSO SST and warm water volume anomalies. *Geophys. Res. Lett.*, **39**, L09706, doi: 10.1029/2012GL051826.

Peng, J. B., L. T. Chen, and Q. Y. Zhang, 2014: The Relationship between El Niño/La Niña cycle and the transition chains of four atmospheric oscillations. Part I: The four oscillations. *Adv. Atmos. Sci.*, **31**(2), 468–479, doi: 10.1007/s00376-013-2275-0. .

Rasmusson, E. M., and T. H. Carpenter, 1982: Variations in tropical sea surface temperature and surface wind fields associated with the Southern Oscillation El Niño. *Mon. Wea. Rev.*, **110**, 354–384.

Schiller, A., J. S. Godfrey, P. C. McIntosh, G. Meyers, and R. Fiedler, 2000: Interannual dynamics and thermodynamics of the Indo-Pacific Oceans. *J. Phys. Oceanogr.*, **30**, 987–1012.

Shi, N., F. Y. Wei, G. L. Feng, and T. L. Sheng, 1997: Monte Carlo test used in correlation and composite analysis of meteorological fields. *Journal of Nanjing Institute of Meteorology*, **20**, 355–359. (in Chinese)

Tourre, Y. M., and W. B. White, 1997: Evolution of the ENSO signal over the Indo-Pacific domain. *J. Phys. Oceanogr.*, **27**, 683–696.

Vialard, J., C. Menkes, J. P. Boulanger, P. Delecluse, E. Guilyardi, M. J. McPhaden, and G. Madec, 2001: A model study of oceanic mechanisms affecting equatorial Pacific sea surface temperature during the 1997-98 El Niño. *J. Phys. Oceanogr.*, **31**, 1649–1675.

Vimont, D. J., J. M. Wallace, and D. S. Battisti, 2003: The sea-

sonal footprinting mechanism in the Pacific: Implications for ENSO. *J. Climate*, **16**, 2668–2675.

Wang, B., 1995: Interdecadal changes in El Niño onset in the last four decades. *J. Climate*, **8**, 267–285.

Weisberg, R. H., and C. Wang, 1997: Slow variability in the equatorial west-central Pacific in relation to ENSO. *J. Climate*, **10**, 1998–2017.

White, W. B., S. C. Chen, R. J. Allan, and R. C. Stone, 2002: Positive feedbacks between the Antarctic Circumpolar Wave and the global El Niño-Southern Oscillation Wave. *J. Geophys. Res.*, **107**, 3165, doi:10.1029/2000JC000581.

Wu, R. G., and L. T. Chen, 1995: 3–5 year time scale evolution of global 1000 hPa height anomaly during 1980–1989. *Chinese J. Atmos. Sci.*, **19**, 575–585. (in Chinese)

Zong, H. F., 2007: Study of impact process of global and local atmosphere anomaly caused by ENSO on precipitation during the Meiyu period. Ph.D. dissertation, Institute of Atmospheric Physics, 109 pp. (in Chinese)